Int. J. Electrochem. Sci., 12 **(2017)** 7341 – 7350, doi: 10.20964/2017.08.69

International Journal of
ELECTROCHEMICAL
SCIENCE
www.electrochemsci.org

Electrochemical Quantitative Detection of Glial Fibrillary Acidic Protein Based on Molecularly Imprinted Polymer Sensor

Tao Wang[1], *Yuan Fang*[2] *and Zhongzheng He*[*]

[1] Department of Neurosurgery, The Central Hospital of Xian, Shanxi Province, Xian, 710004, China
[2] Department of Neurosurgery, The Third Hospital of Xian, Shanxi Province, Xian, 710018, China
[*]E-mail: hezhongzheng68@yeah.net

Received: 6 April 2017 / *Accepted:* 12 June 2017 / *Published:* 12 July 2017

This study synthesized a new glial fibrillary acidic protein (GFAP)-imprinted polymer based on the principle of biomimiking. A carbon electrode printed using an imprinted polymer-modified screen was constructed under 'grafting-to' modification for the detection of the GFAP. Then the atomic force microscopy and scanning electron microscopy assays were employed for the characterization of the decorated surface, with the limit of detection (LOD) of 0.04 μg/mL obtained under aqueous circumstance. The GFAP determination was further investigated in human blood serum to confirm the methodology and effect of the developed sensor.

Keywords: Glial fibrillary acidic protein; Molecularly imprinted polymer; Nervous system; Electrochemical determination; Human blood serum

1. INTRODUCTION

As an intermediate filament (IF) III protein, glial fibrillary acidic protein (GFAP) could be especially detected in non-myelinating Schwann cells in the peripheral nervous system (PNS), enteric glial cells and astrocytes in the central nervous system (CNS). A few lipopolysaccharides (LPSs), growth factors and nuclear-receptor hormones could regulate the expression of GFAP mRNA. Large numbers of post-translational modifications (PTMs) also affect GFAP. The protein deposits termed Rosenthal fibers in Alexander disease is caused by the mutations of the GFAP. The astroglial cell activation (astrogliosis) after CNS injuries and neurodegeneration seems to be greatly affected by the activation of GFAP gene as well as the induction of protein. A fast release of GFAP and its breakdown products into biofluids has been reported to be observed after traumatic brain and spinal cord injuries and stroke; hence they could be recognized as desirable biomarkers for these neurological disorders.

Astrocytes including resident and perivascular microglia, radial glia, oligodendrocytes, and Müller cells are regarded as a sort of glial cell in the CNS. Estimated ss the most adequate cell sorts in the brain, astroglial cells can be used as functional and structural support for neurons. Astrocytes have been determined with GFAP as a distinct structural protein, and the isolation and characterization were performed in 1969 by Dr Eng [1]. It has been well acknowledged that GFAP exists in non-myelinating Schwann cells in the PNS and enteric glial cells as part of the enteric nervous system (ENS) [2, 3]. In this work, the framework of GFAP and varied splice variants of it was initially investigated, along with the pathological importance of GFAP mutations. The mechanism for the regulation of GFAP at the transcriptional and the post-translational levels, the way these regulations influence the normal cytoskeletal functions of GFAP, as well as the engagement in the maintenance of the activated astroglial cell state (astrogliosis) after nervous system injury were also investigated in this work. Then the potential of GFAP and the decorated structures to be a desirable protein biomarker for stroke and neurotrauma was studied. Eventually, the identification of GFAP to be a primary autoantigen after traumatic brain injury (TBI) was studied, along with its potential of inducing a possible post-TBI and maintaining autoimmune response to the nervous system.

Proteolysis and phosphorylation are two primary post-translational modifications in GFAP. They are likely to vary the interpretation of results or for immunoassay standardization. Actually, antibodies specific to the phosphorylated forms of GFAP were employed to study the structural activities of the aforementioned protein. It has been presented that the GFAP immunoreactivity was rapidly varied in cultured astrocytes ascribed to the calcium influx-mediated proteolysis [4, 5].

Normally, a polyclonal anti-GFAP produced from DAKO against bovine GFAP was employed for immunocytochemistry and immunoblotting [6]. The aforementioned antibody has also gained application in other researchers and was effective for the results comparison [7-10]. GFAP in human, rat specimens and other species could be recognized by this antibody. And the immunoblots of rat specimens from cell and tissue culture displayed a single band of 50 kDa. Nevertheless, due to the "quenching" effect of neighboring proteins, immunoblotting used for this antibody showed a GFAP decrease, by comparison with ELISA [9]. But this ELISA was inaccurate and costly. In recent years, electrochemical method has been recognized as a desirable approach for the biological molecule detection [11-18].

A GFAP-imprinted polymer film was fabricated to cover the surface of screen-printed carbon electrodes (SPCEs). A simple method of protein imprinting was fabricated under biologically benign condition, where a multivalent protein complex was polymerized with the polymerizable ligands adsorbed at the surface of the SPCEs. In addition, the electrochemical determination became more sensitive due to the multiwalled carbon nanotubes (MWCNTs) incorporation in coating. Since molecularly imprinted polymers (MIP)-decorated SPCE was simpler, easily and fast prepared, and possessed porous surface, it has been regarded as the optimum electrode for an indirect electrochemical GFAP determination. As mechanically active electrochemical transducers, the aforementioned SPCEs allowed the sensors to be miniaturized, and enabled the integration of the working and reference electrodes in the same chip. In addition, the SPCEs were low-cost. The electroactive probe was potassium ferricyanide/ferrocyanide for the indirect determination of the GFAP. The biomimetic sites were generated onto the surface of the electrode as the GFAP was

extracted, and functioned as accesses for the ferrocyanide to be diffused in and out of the polymeric network. A substitutional electrochemical signal was generated through the oxidization of reduction of the ferrocyanide on the electrode. Due to the stepwise GFAP binding, there was a gradual decrease in the quantity of the potassium ferrocyanide to the surface of the SPCEs. The variation in the reduction peak current intensity of the potassium ferrocyanide on the rebinding of the GFAP was studied using the differential pulse voltammetry (DPV).

2. EXPERIMENTS

2.1. Chemicals

GFAP, 2-aminoethyldihydrogen phosphate, 2,2′-azoisobutyronitrile (AIBN), MWCNTs (internal diameter 2–6 nm, outer diameter 10–15 nm, length 0.2–10 μm, and purity > 90%), N-dimethyl aniline-dihydro chloride, 4-amino-N, ethylene glycol dimethylacryalte (EGDMA), and all interfering agents were commercially available in Sigma–Aldrich. Ethylene diamine tetraacetic acid disodium salt (EDTA), solvents dimethyl sulphoxide (DMSO), potassium ferrocyanide, potassium chloride (KCl), acryclic acid, acryloyl chloride (AC) and sodium-dodecyl sulphate (SDS) were commercially available in Sinopharm Chemical Reagent Co. Ltd. the supporting electrolyte was KCl solution. The solution pH values were adjusted by adding several drops of NaOH (0.1 M) or HCl (0.1 M). Standard stock solution of 50.0 μg/mL GFAP and 5.0 mM potassium ferrocyanide were synthesized by DW.

2.2. Electrode fabrication

The preparation began with covering the pre-activated SPCE using Teflon tape with just the working electrode area free. The pre-polymer mixture (8.0 μL) consisted of MWCNTs (20.0 mg), initiator (AIBN; 0.09 mg/1.0 mL DMSO), and monomers (DMAA and AEDP; each 0.5 mg/1.0 mL DMSO), as well as cross-linker and the template, respectively, 400 μL EGDMA and 0.05 mg/50 μg/mL GFAP. After spin coating onto the working electrode, and spinning at 2000 rpm for 0.5 min, this mixture was thermally polymerized at 40 °C, and then MIP was grafted onto the surface of the SPCE. This was followed by spinning coating the hot agarose solution (10.0 μL, 2% (w/v)) in DW onto the decorated electrode, along with 2500 rpm spinning for 40 s, and then a thin layer of agarose was formed. This layer was heated at 30 °C to generate a stable thin membrane over the electrode. The MIP polymer grafted onto the SPCE turned more stable with the presence of this agarose film. The Teflon tape was removed from the SPCEs, after the agarose was dried. After immersion in SDS (10% (w/v)) and HCl mixture (0.1 N) for 4 h, the decorated SPCEs were treated with EDTA (0.5 M) for 60 min to extract the template. The appearance of a minimal peak current for potassium ferrocyanide in KCl supporting electrolyte (0.1 M) indicated that the template had been thoroughly removed out of the MIP-adduct. A non-imprinted polymer (NIP) film was synthesized with the same route, just except for the absence of GFAP.

2.3. Characterizations

Fourier transform infrared spectra (FTIR) were obtained using a Bruker Vertex 70 spectrometer. A CHI 660D electrochemical workstation (CH Instruments, Shanghai, China) was employed for all electrochemical tests. The triple-electrode configuration consisted of bare or modified SPCE, saturated calomel electrode (SCE) and a platinum wire, respectively as the working, reference and auxiliary electrode. All the electrochemical assays were carried out at ambient temperature with potassium ferrocyanide (5.0 mM)-spiked KCl (10.0 mL, 0.1 M). Nevertheless, potassium ferrocyanide (1 mM)-spiked KCl (200.0 μL) was employed as the supporting electrolyte, especially for the determination of real specimens. The analyte accumulation was performed at +0.5 V for 2 min prior to DPV and CV measurements. The potential window with a range of +0.6 to −0.3 V was applied to CV measurements, while a range of +0.3 to −0.2 V was applied to DPV measurements (scan rate: 10 mV/s^{-1}; pulse amplitude: 25 mV). After immersing the as-prepared electrodes to the aforementioned electrolyte containing potassium ferrocyanide, GFAP was spiked with varied concentrations for electrochemical assays. Because of the template intake and probe molecule (Fe(III), oxidized form at +0.5 V) release, there was current response variation, which was plotted against template concentration for regression determination. It was unessential for the cell content to be de-aerated for the dissolved oxygen in the cell caused no influence on the current response. To evaluate the imprinting efficiency of polymer, this work also constructed the SPCEs and NIP/SPCEs, which were later studied under the same experimental conditions as that of MIP/SPCEs.

3. RESULTS AND DISCUSSION

The heterogeneous reactions during the quasi-reversible or irreversible redox processes show slower kinetics due to the high amounts of polymer in terms of SPCEs fabrication. Hence the SPCEs are essential to be activated through moderate electrochemical activating methods to optimized the electrochemical behavior [19]. The bare SPCEs receive a short electrochemical pre-anodization treatment at a high positive polarization potential, and then there is an increase in their surface roughness and functionalities, as well as the surface contaminants removal, which would further lead to an increase in the heterogeneous transfer constant for the $[Fe(CN)_6]^{4-}/[Fe(CN)_6]^{3-}$ couple, as well as the enhanced electrochemical reversibility and analytical behavior.

Fig. 1 indicated that a characteristic reversible $Fe^{2+/}Fe^{3+}$ redox response was observed for the SPCEs, where the cathode peak suggested that Fe^{3+} was reduced back to Fe^{2+}, while the anodic peak indicated $Fe^{2+}$was oxidized. As the SPCE was modified using the NIP/MIP polymer, a layer was produced as a barrier that led to the physical blocking of the surface of the electrode for ferricyanide/ferrocyanide reduction/oxidation. Hence it can be expected that there would be a significant current decrease onto the modified electrode than the unmodified electrode. The NIP/SPCE showed the nearly identical effect, while the probe molecule displayed basically no current response due to the lack of cavity. Nevertheless, an extremely desirable current response was obtained for the MIP/SPCE to the probe molecule, while lower compared with that of the unmodified electrode. There

was an obvious current response for MIP/SPCE since the cavities existed onto the surface of the electrode, functioning as routes for easy approach of the probe molecule to the electrode surface prior to the exposure to template analyte. The apparent coverage of polymer on the surface of the bare electrode was approximated using the relative current ratio of the two anodic/cathodic peaks on MIP/SPCE and the unmodified electrode obtained at constant potential, with the apparent surface coverage of MIP/SPCE was calculated as 27.4%. The low % value indicates that the MIP layer was highly porous, while not suggesting the undesirable polymer-involved surface coverage herein.

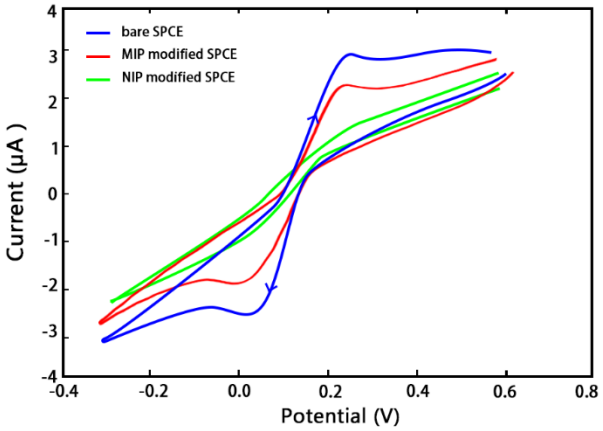

Figure 1. CV characterizations for the SPCEs, MIP/SPCEs and NIP/SPCEs in potassium ferrocyanide solution (0.05 mM) which contains KCl supporting electrolyte (0.1 M, pH 7.0) at the SPCEs, MIP/SPCEs and NIP/SPCEs.

Generally, the protein backbone showed two most significant vibration bands: amide I and II bands [20]. The amide I band (1700–1600 cm^{-1}) ascribed to the C=O stretch vibrations of the amide coupled with C—N stretching and in-plane N—H banding in peptide linkages was more significant, but for the characterization of secondary structure of protein. By comparison, the amide II band was formed primarily due to the NH bending and the CN stretching vibration of proteins amide species. The GFAP - Ca^{2+} binding was indicated by the bands observed at 435 cm^{-1} (Ca^{2+}—O bond) and 722 cm^{-1} (Ca^{2+} and COO^{-} group of amino acid), as indicated in the FTIR characterization of GFAP in Fig. 2. These bands were characteristic of the template molecule. The tentative binding mechanism between template and monomer(s) was found with the comparison among the FTIR characterizations of MIP, MIP-template adduct and the template. The monomer (DMAA) [3442 (ν_s NH), 1727 (—C=O), 1374 cm^{-1}(δ C—N)], phosphate monomer (AEDP) [3463 (—N—H), 1740 (C=O), 1640 (amide I), 1565 (amide II), 1421 (P=O), 983 cm^{-1} (p-OH)], and amino acid moieties present in GFAP [3392 (super-imposed O—H and NH_3^{+}) corresponded to the IR bands. The phosphate (AEDP) - Ca^{2+} (GFAP) interaction explained the emergence of novel wide band in MIP-template adduct at 540–620 cm^{-1}[21]. The interaction between phenyl ring of monomer and phenyl substituted amino acids in the template was indicated by the decrease in monomer and template bands from 1235, 1122, and 1160, 1125 cm^{-1} to 1150 and 1122 cm^{-1}. All the varied bands turned back to original state after the template was retrieved. MIP displayed the FTIR bands at 720 and 438 cm^{-1}, suggesting that the template was completely removed out of the MIP-template adduct. The MIP-template adduct-extracted template

shared similarity with the bare GFAP molecules in their FTIR bands, indicating the stability of the GFAP in pre-polymer mixture, and that the MIP preparation was performed in biologically benign condition, producing no denatured GFAP during polymerization.

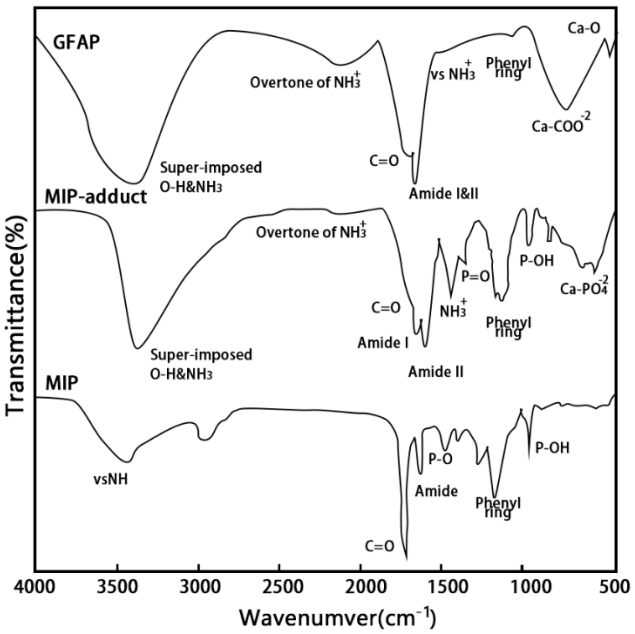

Figure 2. FTIR characterization of GFAP, MIP-adduct and MIP.

After the immersion in the voltammetic cell which contained KCl (10.0 mL) and ferrocyanide (0.19 mM), the MIP/SPCE was successfully pre-treated for the electrochemical tests. This was followed by introducing 50.0 μg/mL GFAP solution to the aforementioned cell. With the recombination of GFAP by the imprinted sites under ion-transfer, the access of ferrocyanide probe molecules via molecular cavities to the surface of the electrode was limited. Actually, the imprinted sites of GFAP macromolecules could not be inhabited since ferrocyanide probe was small. Instead, an easier approach could be found via the cavity to the surface of the electrode. The obstruction of these accesses of probe was activated by the binding affinity of GFAP molecules, and then led to a gradual decrease in the electrochemical signal, as GFAP encapsulation was increased in MIP-cavities. This phenomenon was recorded using DPV and CV methods, as shown in Fig. 3A and Fig. 3B, respectively. Despite of similar desirable response to GFAP addition, DPV was found comparatively more sensitive than CV, hence DPV was selected to quantitatively detect GFAP in this work.

As the GFAP concentration increased, there was a gradual decrease of the current, which eventually turned steady at over 8.5 μg/mL achieved by the saturation of the binding sites. The NIP/SPCEs showed no signal, even when the target analyte increased in concentration. This phenomenon indicated that the imprinting effect was important in forming molecular cavities, where GFAP – ferrocyanide (probe) anions ion transfer process contributed to the facilitation of the binding. The LOD was calculated as 0.04 μg/mL. The sensitivity of the proposed sensor was compared with that of other reported GFAP sensors and the results were presented in Table 1.

Table 1. Comparison of the present electrochemical sensor with other GFAP determination methods.

Method	Linear detection range	Detection limit	Reference
ELISA	0-14 ng/mL	0.79 ng/mL	[22]
ELISA	500 -1300 pg/mL	200 pg/mL	[23]
Enhanced lanthanide fluorescence immunoassay	0.5–2 μg/mL	0.2 μg/mL	[24]
NIP/SPCEs	0.2-10 μg/mL	0.04 μg/mL	This work

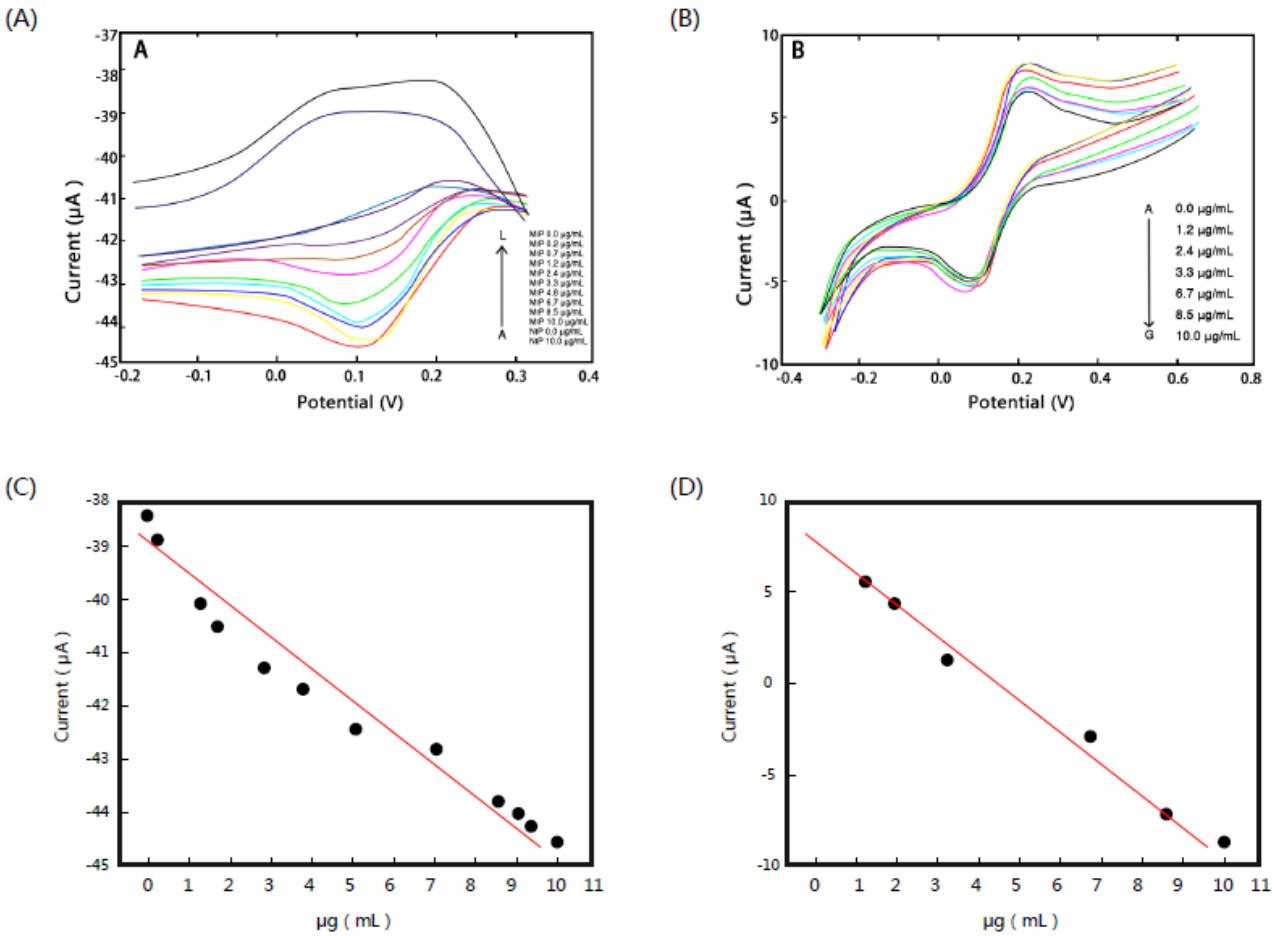

Figure 3. (A) DPV response for MIP/SPCEs and NIP/SPCEs after injecting GFAP solution to the background electrolyte. The terminal concentrations for GFAP: MIP (0.0, 0.2, 0.7, 1.2, 2.4, 3.3, 4.8, 6.7, 8.5, 10.0 μg/mL) and NIP/SPCEs (0.0, 10.0 μg/mL). (B) CV response under same condition as that of DPV for MIP/SPCEs. The terminal concentration for GFAP: 0.0, 1.2, 2.4, 3.3, 6.7, 8.5 and 10.0 μg/mL. (C) Calibration curve of NIP/SPCEs recorded from DPV towards different concentrations of GFAP. (D) Calibration curve of NIP/SPCEs recorded from CV towards different concentrations of GFAP.

To validate the developed sensor in real sample detection, different specimens of varied patients have been investigated, with corresponding results shown in Table 2. An ELISA kit (NS830 - EMD Millipore) has been purchased for comparison. This sensor has the potential to be used for GFAP biomarker in human blood serum, since it has been confirmed that the developed sensor is applicable to GFAP content detection for all cases with a wide range of concentration. It has been well acknowledged that the GFAP concentration is likely to be as high as 20–40 μg mL^{-1} in the case of viral infections, even reaching 500 μg mL^{-1} in the case of bacterial infections, thus it is necessary for the specimen to be diluted with water prior to quantitative analysis. This diluting treatment could move the detection in the range (0.2–8.50 μg/mL) of the developed sensor, as well as facilitate the mitigation of any possible matrix complication for real specimens.

Table 2. Analytical data of DPV assays on MIP/SPCEs and NIP/SPCEs for GFAP in blood serum in varied patients.

Sample	NIP-SPCEs	MIP-SPCEs	Addition	Found	ELISA	Recovery	RSD
1	—	0.85 μg/mL	2 μg/mL	2.87 μg/mL	2.86 μg/mL	100.70 %	4.7 %
2	—	1.44 μg/Ml	2 μg/mL	3.40 μg/mL	3.34 μg/mL	98.84 %	2.3 %
3	—	2.51 μg/mL	2 μg/mL	4.54 μg/mL	4.52 μg/mL	100.67 %	3.3 %
4	—	0.98 μg/mL	2 μg/mL	3.05 μg/mL	3.07 μg/mL	102.35%	1.8 %

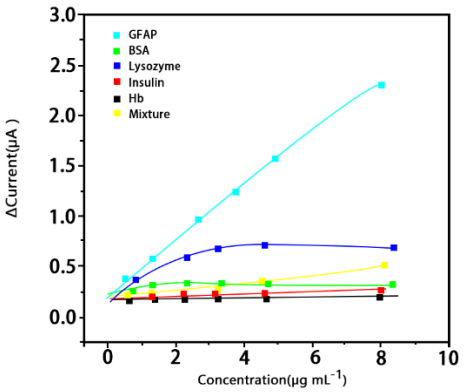

Figure 4. The plots of diminished current changes on MIP-modified SPCEs after addition (concentration range 0.1–8.50 μg/mL) of GFAP, BSA, lysozyme, insulin, Hb, and mixture in 0.1 M KCl (pH = 7.0).

Lysozyme, haemoglobin (Hb), insulin, and bovine serum albumin (BSA) were selected as the interfering agents in a concentration range of 0.1 - 8.50 μg/mL for the evaluation of the MIP/SPCE. Compared with other proteins, an extremely sensitive response to GFAP was observed for the MIP/SPCE (Fig. 4), indicating that the GFAP was specifically integrated to the complementary sites in

the imprinted polymer. There was an obvious decrease in the peak current intensity of potassium ferrocyanide (Fig. 4), suggesting that as soon as the GFAP was added to 8.50 μg/mL, there was a linear increase of the current. The reasonable current drop observed at lower concentration may be ascribed to the nonspecific contribution of interference binding to the recognition sites. The ratio of the original linear gradient variation of GFAP peak current – interfering agents like S_1/S_2 could be evaluated to investigate the selectivity of the MIP/SPCE [25]. And the GFAP selectivity factors on the MIP/SPCE with BSA and mixture have been obtained respectively as 15.2 and 4.8, indicating the more desirable sensitivity of the MIP/SPCE to GFAP than other interfering agents.

4. CONCLUSIONS

This work fabricated an electrochemical biosensor that possessed desirable selectivity and specificity for GFAP determination using surface imprinting technique. One of the monomers (AEDP) was employed to substitute the original binder to simulate the biological GFAP – polymer binding. As a tertiary ammonium group containing monomer, DMAA was also employed to engage in the non-covalent interaction with the negatively charged GFAP molecules. All measurements were performed with precise and accurate data obtained at μg/mL level, not including any possible non-specific false positive contributions and cross-reactivity interference.

References

1. L. Eng, R. Ghirnikar and Y. Lee, *Neurochemical Research*, 25 (2000) 1439.
2. B. Gulbransen and K. Sharkey, *Nature Reviews Gastroenterology and Hepatology*, 9 (2012) 625.
3. C. Laranjeira, K. Sandgren, N. Kessaris, W. Richardson, A. Potocnik, P. Berghe and V. Pachnis, *The Journal of Clinical Investigation*, 121 (2011) 3412.
4. N. Inagaki, K. Tsujimura, J. Tanaka, M. Sekimata, Y. Kamei and M. Inagaki, *Neurochemical Research*, 21 (1996) 795.
5. Y. Lee, S. Du, H. Rhim, E. Lee, G. Markelonis and T. Oh, *Brain Research*, 864 (2000) 220.
6. D. Ziegler, D. Oliveira, C. Pires, L. Ribeiro, M. Leite, A. Mendez, D. Gonçalves, F. Tramontina, L. Portela and S. Wofchuk, *Neuroscience Research*, 50 (2004) 375.
7. S. Guo-Ross, E. Yang, T. Walsh and S. Bondy, *Journal of Neurochemistry*, 73 (1999) 1609.
8. M. Hollborn, S. Tenckhoff, K. Jahn, I. Iandiev, B. Biedermann, U. Schnurrbusch, G. Limb, A. Reichenbach, S. Wolf and P. Wiedemann, *Mol Vis*, 11 (2005) 397.
9. J. O'Callaghan, H. Imai, D. Miller and A. Minter, *Analytical Biochemistry*, 274 (1999) 18.
10. W. van Geel, H. de Reus, H. Nijzing, M. Verbeek, P. Vos and K. Lamers, *Clinica Chimica Acta*, 326 (2002) 151.
11. D. Kumar and B. Prasad, *Sensors and Actuators B: Chemical*, 171–172 (2012) 1141.
12. V. Adam, D. Chudobova, K. Tmejova, K. Cihalova, S. Krizkova, R. Guran, M. Kominkova, M. Zurek, M. Kremplova and A. Jimenez, *Electrochimica Acta*, 140 (2014) 11.
13. S. Shrestha, R. Mascarenhas, O. D'Souza, A. Satpati, Z. Mekhalif, A. Dhason and P. Martis, *Journal of Electroanalytical Chemistry*, 778 (2016) 32.
14. M. Amiri, H. Salehniya and A. Habibi-Yangjeh, *Ind. Eng. Chem. Res.*, 55 (2016) 8114.
15. S. Singal and A. Srivastava, *Nano-Micro Letters*, 9 (2017) 7.
16. R. Soomro, K. Hallam, Z. Ibupoto, A. Tahira, S. Jawaid, S. Sherazi and M. Willander, *RSC*

Advances, 5 (2015) 105090.
17. D. Kumar, D. Manoj and J. Santhanalakshmi, *Analytical Methods*, 6 (2014) 1011.
18. M. Balamurugan, T. Madasamy, M. Pandiaraj, K. Bhargava, N. Sethy and C. Karunakaran, *Analytical Biochemistry*, 478 (2015) 121.
19. J. Wang, M. Pedrero, H. Sakslund, O. Hammerich and J. Pingarron, *The Analyst*, 121 (1996) 345.
20. J. Kong and S. Yu, *Acta Biochimica et Biophysica Sinica*, 39 (2007) 549.
21. F. Miller and C. Wilkins, *Anal. Chem*, 24 (1952) 1253.
22. M. Honda, R. Tsuruta, T. Kaneko, S. Kasaoka, T. Yagi, M. Todani, M. Fujita, T. Izumi and T. Maekawa, *Journal of Trauma and Acute Care Surgery*, 69 (2010) 104.
23. L. Rosengren, C. Wikkelsø and L. Hagberg, *Journal of Neuroscience Methods*, 51 (1994) 197.
24. U. Missler, M. Wiesmann, G. Wittmann, O. Magerkurth and H. Hagenström, *Clinical Chemistry*, 45 (1999) 138.
25. G. Poirier and E. Pylant, *Science*, 272 (1996) 1145.